

This Page Is Inserted by IFW Operations  
and is not a part of the Official Record

## **BEST AVAILABLE IMAGES**

Defective images within this document are accurate representations of the original documents submitted by the applicant.

Defects in the images may include (but are not limited to):

- BLACK BORDERS
- TEXT CUT OFF AT TOP, BOTTOM OR SIDES
- FADED TEXT
- ILLEGIBLE TEXT
- SKEWED/SLANTED IMAGES
- COLORED PHOTOS
- BLACK OR VERY BLACK AND WHITE DARK PHOTOS
- GRAY SCALE DOCUMENTS

**IMAGES ARE BEST AVAILABLE COPY.**

**As rescanning documents *will not* correct images,  
please do not report the images to the  
Image Problem Mailbox.**

### **REMARKS**

Applicant considered the Office Action mailed on October 22, 2003, and the references cited therewith. This response cancels claims 32 and 42 without prejudice, amends claims 2, 33-34, 37, and 43-44, and adds new claims 45-55. As a result, claims 2-8, 33-41, and 43-55 remain pending in the Application.

### **§112 Rejections of the Claims**

Claims 2-8 and 32-44 were rejected under 35 USC §112, first paragraph, as failing to comply with the written description requirement. Applicant respectfully traverses these rejections.

When Applicant employs the word “seamless,” it is abundantly clear that she means it in an optical sense, and this sense was apparently understood through three Office actions dealing with claims that included this term. For example, the two terms “seamlessly” and “without visible seam” are equated as synonyms<sup>1</sup> at page 6 lines 17-22 of the Specification. Nevertheless, claims 2 and 37 are amended so as to recite explicitly that the tiling is without a “visible” seam. It is of course impossible to show directly in Fig. 7 a seam which is invisible. However, the description of Fig. 7 at page 6 lines 23-28 clearly says that it is “seamlessly tiled” (line 27). And, in any case, Fig. 6 explicitly indicates multiple seamlessly tiled faceplates 10, described in the Specification at page 5 lines 10-20. Note especially the plural reference to “faceplates 10” in line 20.

Because the amendments to claims 2 and 37 merely replace one term with another equivalent term, they do not narrow the scope of the claims.

New claims 45-56 do not include recitations to seams or their absence, and thus entirely avoid any grounds for rejection under 35 USC §112.

### **§103 Rejections of the Claims**

Claims 2-8, 32-38 and 42-44 were rejected under 35 USC §103(a) as being unpatentable over Sakai et al. (U.S. 5,502,457) in view of *Adventures in Fiber Optics Kit* by Industrial Fiber

---

<sup>1</sup> ---It is well settled that an applicant may be his own lexicographer, and may employ terms that modify a dictionary definition, as long as their use does not contravene a meaning that is standard in the applicable technology.

Optics, Inc. (AFOK) Applicant respectfully traverses these rejections. Applicant's previous responses have adduced reasons that the claims distinguish the references. This response is accordingly limited to the points raised in paragraphs 7-12 of the Office Action.

Paragraph 7 states that "the examiner doesn't use Sakai's reference to overcome said limitation" to fibrous crystalline material. However, the rejection under 35 USC §103 is based upon a combination of the Sakai reference with the AFOK reference. Therefore, 35 USC §103 requires that Sakai must provide some internal motivation for using other than the conventional glass fibers that he shows. Applicant has discovered a novel property of certain materials, a lack of "dead fibers" (see page 3 lines 1-3) at the edges that allows these materials to be tiled (optically) seamlessly very easily and cheaply, whereas conventional fibers such as Sakai proposes requires special techniques for multiple use. Thus, the rejection has impermissibly combined Sakai and AFOK only in light of Applicant's disclosure.

Applicant does not understand how AFOK suggests any combination whatsoever of individual faceplates with each other. The statement in paragraph 8 of the Office Action only speaks of and shows individual faceplates. The only motivation for tiling such individual faceplates spring from Applicant's inventive recognition that these materials, unlike other optical materials, do not have dead fibers at the edge that produce optically objectionable joints or seams. AFOK certainly contains no hint of Applicant's insight, and thus has no motivation for tiling multiple individual faceplates.

As to the "scale of nanometers" in paragraph 9, Applicant reiterates the common understanding that this phrase would not be taken by anyone in the art to refer to tens of thousands of nanometers. In addition, however, the Specification provides a basis for quantifying this term more closely. Page 6 lines 18-20 equates this scale to the size of the optical channels in the material: "A faceplate made of fibrous crystal in accordance with the present invention would have a pitch or fiber size on a scale of nanometers and therefore would produce no visible seam." This quantity is known in the art. For example, the attached copy of Ikhuvara et al., *Microstructure characterization of one-directionally oriented ulexite*, J. Mater. Res. vol. 43 no. 3 (Mar. 1998), pp. 778-783 states on page 779 col. 2 that "average grain size of the

bundles is several tenths  $\mu\text{m}$ .” That is, several hundred nanometers.<sup>2</sup> This is smaller by two orders of magnitude than the 30,000nm in the reference.

As to paragraph 10, the fact that “Ulexite ... may one day be refined and used commercially” does not say or suggest---except in the knowledge of Applicant’s disclosure---that it can be manufactured in a laboratory. “Refining” a mineral or an ore denotes purifying it from a natural state, and does not imply “producing” it from its constituents in a laboratory or manufacturing facility. Certainly AFOK suggests no advantage of a synthetic version. Applicant, in contrast, proposes several advantages of a lab-grown version in some environments; see page 6 lines 5-17 of the Specification, for example. Thus, AFOK bare statement that sometime in the indefinite future someone might possibly find some unspecified use for a purified form of the natural mineral, does not amount to a motivation to synthesize it from its constituents.

See new claim 48 in connection with paragraph 10.

The comments in paragraph 12 appear moot, because this Office Action does not reject any claims on the previously cited Bilbro reference. The only rejections under 35 USC §103 appear to be claims 2-8, 32-38, and 42-44 as to Sakai and AFOK, in paragraph 4 of the Office Action. However, the reasoning in paragraph 12 is specious in any event. Claim 37 recites the “image source” from the “first diffusing assembly” as separate elements. If Applicant’s “light source” is read on the combination of Sakai’s light source and his fiber bundles, then Sakai has no other distinct element that can be applied to Applicant’s “first diffusing assembly” with its tiled crystals.

### **New Claims**

New independent claims 45 and 53 do not include seamless tiling. Therefore, they escape any rejection of claims 2 or 37 under the first paragraph of 35 USC §112. Further, as demonstrated above and in previous responses, claim 2 distinguishes the cited references any valid combination thereof without recourse to seamlessness of the tiling.

---

<sup>2</sup> ---Additional support for this range of values lies in the last part of the passage quoted from the Specification. The lack of visible seam arises from the fact that the fiber size is commensurable with the wavelengths of visible light. One skilled in the optical arts would be expected to know this.

Dependent claims 46-52 and 54-55 incorporate the features of their parents, and distinguish the references as well. In particular, claim 49 specifies that the optical faceplate is “doped so as to change its optical properties,” the advantages of which are described on page 6 lines 5-12 of the Application. Sakai mentions Ulexite not at all, and AFOK suggests no doping of the natural crystal material, nor any conceivable reason for doing so. As other examples, claims 50-52 recite other modifications to synthetic crystals, modifications that are not found in nature. Page 5 lines 12-14 discusses these modifications. None of them are even remotely suggested in the cited references.

Dependent claim 47 omits Ulexite from the claimed group of “Selenite, Artinite and Aragonite,” and thus avoids any materials shown in or suggested by the cited references. Dependent claim 55 recites that the fibrous crystal has a pitch “less than that of glass.” Glass, of course, is the material employed by Sakai, and Sakai has no suggestion of or motivation for, using a material with a smaller pitch.

AMENDMENT AND RESPONSE UNDER 37 CFR § 1.111  
Serial Number: 09/751357  
Filing Date: December 29, 2000  
Title: SEAMLESS REAR PROJECTION SCREEN

Page 10  
Dkt: 256.063US1

Conclusion

For the above and other reasons, Applicant urges that the Application meets all statutory requirements, and respectfully requests reexamination under 35 USC §132 and allowance of the claims. The Examiner is invited to telephone Applicant's attorney at (612) 373-6971 if deemed desirable to facilitate prosecution of this Application.

If necessary, please charge any additional fees or credit overpayment to Deposit Account No. 19-0743.

Respectfully submitted,

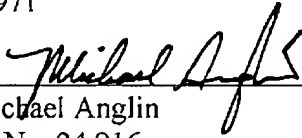
ALEKSANDRA KOLOSOVSKY

By her Representatives,

SCHWEGMAN, LUNDBERG, WOESSNER & KLUTH, P.A.  
P.O. Box 2938  
Minneapolis, MN 55402  
(612) 373-6971

Date 22 Jan 2004

By

  
J. Michael Anglin  
Reg. No. 24,916

CERTIFICATE UNDER 37 CFR 1.8: The undersigned hereby certifies that this correspondence is being deposited with the United States Postal Service with sufficient postage as first class mail, in an envelope addressed to: Commissioner of Patents, P.O. Box 1450, Alexandria, VA 22313-1450, on this 22 day of January, 2004.

Gina M. Uphus

Name

  
Signature

## Microstructure characterization of one-directionally oriented ulexite

Yumi H. Ikubara and Shinji Kondoh

Synergy Ceramics Laboratory, Fine Ceramics Research Association, 2-4-1 Mutsuno, Aizawa-ku, Nagoya 456, Japan

Koichi Kikuta

National Industrial Research Institute of Nagoya, 1 Hirate-cho, Kita-ku, Nagoya 462, Japan

Shin-ichi Hirano

Department of Applied Chemistry, School of Engineering, Nagoya University, Furo-cho, Chikusa-ku, Nagoya 464-01, Japan

(Received 22 February 1997; accepted 23 May 1997)

Microstructures of ulexite were investigated by CTEM and low electron dose HREM. It was found that the longitudinal grains in ulexite were oriented to *c*-direction to form a bundle structure. There were a number of small-angle grain boundaries and stacking faults inside a grain in the ulexite. Cleavage microcracks and stacking faults were mostly introduced on the {010} of the ulexite. The high-angle grain boundaries mainly consisted of high coincidence boundaries, which was confirmed by a comparison of observed contact angles and calculated degree of coincidence at the boundaries. The light transmittance properties of the ulexite would depend on the defects such as stacking fault, small-angle grain boundary, and high-angle grain boundary.

### INTRODUCTION

As the media of light transmission, optical fibers have been intensively studied for several decades.<sup>1-4</sup> The optical fibers are usually amorphous and consist of the characteristic microstructure such as clad and core with different refractive indices. On the other hand, ulexite discovered in nature has a unique optical property as the media of light transmission. Ulexite transmits the light along an oriented direction, and thus is called "television line." Ulexite has an optically biaxial positive crystal and has refractive indices  $\alpha = 1.49$ ,  $\beta = 1.504$ , and  $\gamma = 1.520$ .<sup>5</sup> If the refractive indices of the neighboring fiber are  $\alpha$  and  $\gamma$ , the boundary of the fiber is separated into the high and low index region, thus the high index end of the fiber behaves as the clad compared to the low index plane of the neighboring fiber.<sup>6</sup> Therefore, one elongated crystal of ulexite has a function as an optical fiber. The light traveling from one side of the elongated section of the bundle transmits through the crystal to the opposite side, repeatedly the total reflection at the boundary of the crystals with different refractive indices.

Ulexite has a triclinic structure ( $a = 8.809$  Å,  $b = 12.86$  Å,  $c = 6.678$  Å,  $\alpha = 90.15^\circ$ ,  $\beta = 109.07^\circ$ ,  $\gamma = 105.06^\circ$ ), and the oriented microstructure of the bundle is parallel to the *c*-axis. Its transmittance property depends on the microstructure such as grain boundary and stacking fault inside the crystal. The crystal structure of ulexite has been identified using x-ray diffraction analysis<sup>7-9</sup>; however, XRD technique provides only

average structures in the materials. In order to have a full understanding of the properties, another technique is needed to observe local structures such as lattice defects.

High resolution electron microscopy (HREM) is one of the most effective methods for characterizing local microstructures with an atomic scale. However, no attempt has been made to characterize ulexite by HREM and even by conventional TEM (CTEM). This is because the ulexite is too unstable to observe under the electron beam irradiation.<sup>10</sup> The chemical composition of ulexite is  $\text{NaCaB}_3\text{O}_6(\text{OH})_6 \cdot 5\text{H}_2\text{O}$ ,<sup>11,12</sup> and thus, the combined water is included inside the structure. The existence of the water does not enable us to observe an image under ordinary conditions of CTEM and HREM observations (beam current density  $>10$  A/cm<sup>2</sup>).

In this study, we used mainly a technique of low electron dose HREM to characterize the microstructure of ulexite. In addition to HREM, selected-area diffraction patterns (SADP's) and CTEM were utilized to investigate the grain structure such as crystal orientation, grain boundaries, and stacking faults in ulexite. Grain boundary characteristics are discussed on the basis of the observed results.

### II. EXPERIMENTAL PROCEDURE

The ulexite sample analyzed in this study was obtained from California. First, x-ray powder diffraction analysis was carried out to confirm the crystal structure of ulexite using a Rint2000 (Rigaku Co. Ltd.) x-ray

fractometer with  $\text{Cu K}\alpha$  radiation. Next, the morphology of the ulexite was observed with the electron microscope (S-800, Hitachi Co. Ltd.) to evaluate the grain size and distribution.

Specimens were prepared using standard technique involving mechanical grinding to a thickness of up to a thickness of  $20\text{ }\mu\text{m}$ , and ion beam electron transparency at  $3\text{--}4\text{ kV}$ . The ion mill (Dual Ion Mill Model 600, Gatan Co. Ltd.) using a cold stage cooled by liquid  $\text{N}_2$  to avoid the specimens. The sample was subsequently polished by a JEM4000FX (JEOL Co. Ltd.) electron microscope operated at  $400\text{ KeV}$ . HREM observations were made to minimize the electron dose using high magnification. The electron dose used for the present study was less than about  $0.05\text{ A/cm}^2$ , which is less than  $<1/200$  of that for the ordinary HREM studies. Thus, the direct magnification was as small as  $100\times$ , and the exposure time was as long as  $5\text{--}7\text{ s}$ .

SADP's were also taken at an electron dose of  $0.05\text{ A/cm}^2$ . Both the TEM and SEM observations were performed with the incident beam parallel to the  $c$ -axis of the ulexite crystal.

## RESULTS AND DISCUSSION

Figure 1 shows the x-ray diffraction pattern of the crushed ulexite powder. All diffraction peaks can be indexed by the diffraction indices calculated from the structure of ulexite with  $P\bar{1}$  space group and  $a = 12.86\text{ }\text{\AA}$ ,  $b = 6.678\text{ }\text{\AA}$ ,  $c = 90.15^\circ$ ,  $\alpha = 7^\circ$ , and  $\gamma = 105.06^\circ$ . The strong peak at  $2\theta =$

$7.24^\circ$  corresponds to the  $b$ -plane with the interplanar distance of  $d = 1.22\text{ nm}$ .

Figure 2 shows a SEM micrograph of the surface of ulexite. The surface of the specimen is perpendicular to the oriented structure which is parallel to the transparent direction. As seen in the figure, ulexite is composed of fiber bundles parallel to the  $c$ -direction, and the average grain size of the bundles is several tenths  $\mu\text{m}$ . The white contrast in each grain corresponds to microcracks inside a grain. The direction of the microcracks in one grain is approximately aligned in parallel, which suggests the  $\{010\}$  cleavage plane of ulexite.<sup>5</sup> Each grain contacts with the neighbor grains at some specific contact angles, which will be discussed in detail later.

The chemical analysis in a grain and near grain boundary was done by energy dispersed x-ray spectroscopy (EDS). It was found that the composition was uniform and there were no precipitates in the grain boundaries.

Figure 3 shows SADP's taken from the (a)  $\langle 001 \rangle$  zone axis and (b)  $\langle 010 \rangle$  zone axis. In Fig. 3(a), the streak can be observed along the  $[010]$  direction, which suggests the formation of stacking faults on the  $\{010\}$  planes.

Figure 4 shows a (a) HREM image observed along the  $[001]$  direction, and (b) the filtered image of (a). The filtered image was obtained by Fast Fourier Transformation (FFT) of the original image in a computer. The lattice images of  $(100)$  and  $(010)$  are clearly observed in the figures. The interplanar spacings and angles are consistent with triclinic structure of ulexite projected along the  $c$ -direction.

Figure 5 shows a bright-field TEM image and SADP's observed nearly along the  $\langle 001 \rangle$  direction of

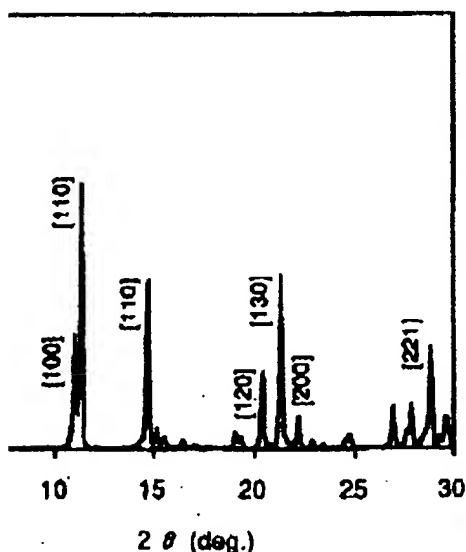


Fig. 1. X-ray diffraction pattern from the crushed ulexite powder.



Fig. 2. Scanning electron micrographs on the surface of ulexite observed from the vertical direction along the oriented fibers. White contrast indicates the microcracks along the grain boundary.



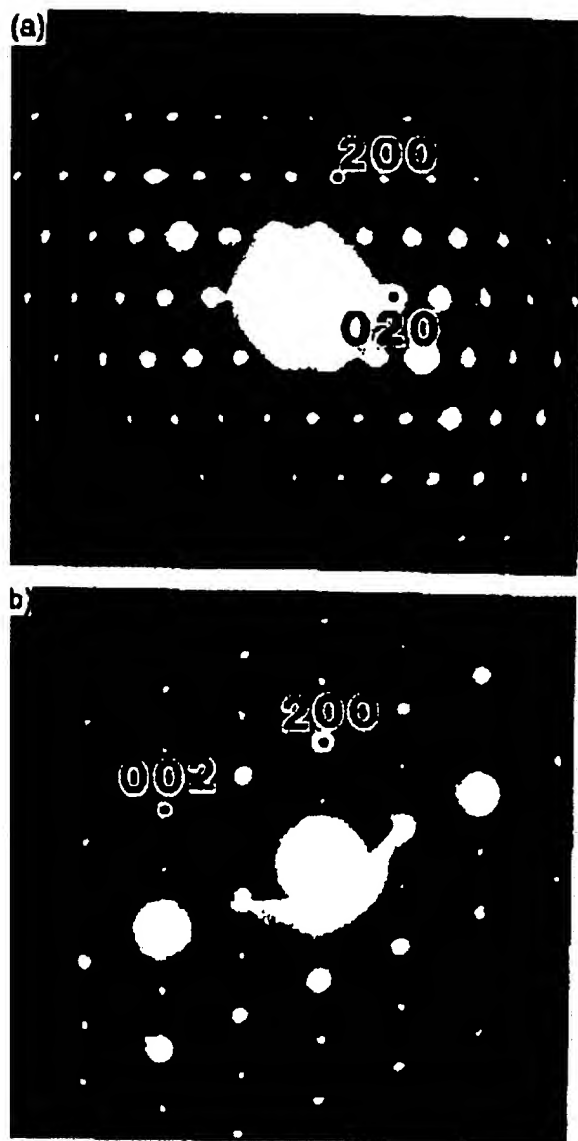


FIG. 3. SAD patterns taken from the (a) (001) zone axis and (b) (010) zone axis.

exit. The SADP's of 1-6 were taken from the  $0.5 \mu\text{m}$  area of the same number in the TEM micrograph. The set represents the diffraction pattern of 1. Each SADP set so as to take orientation to the TEM micrograph. It thus found that the microcracks are introduced parallel the {010} planes. This is consistent with the results Murdoch that the cleavage plane of ulexite is a {010} plane.<sup>5</sup> The large interplanar spacing of 1.22 nm might be the reason for the cleavage property of {010} planes. Mechanical polishing of the sample is considered to induce a number of microcracks along the cleavage

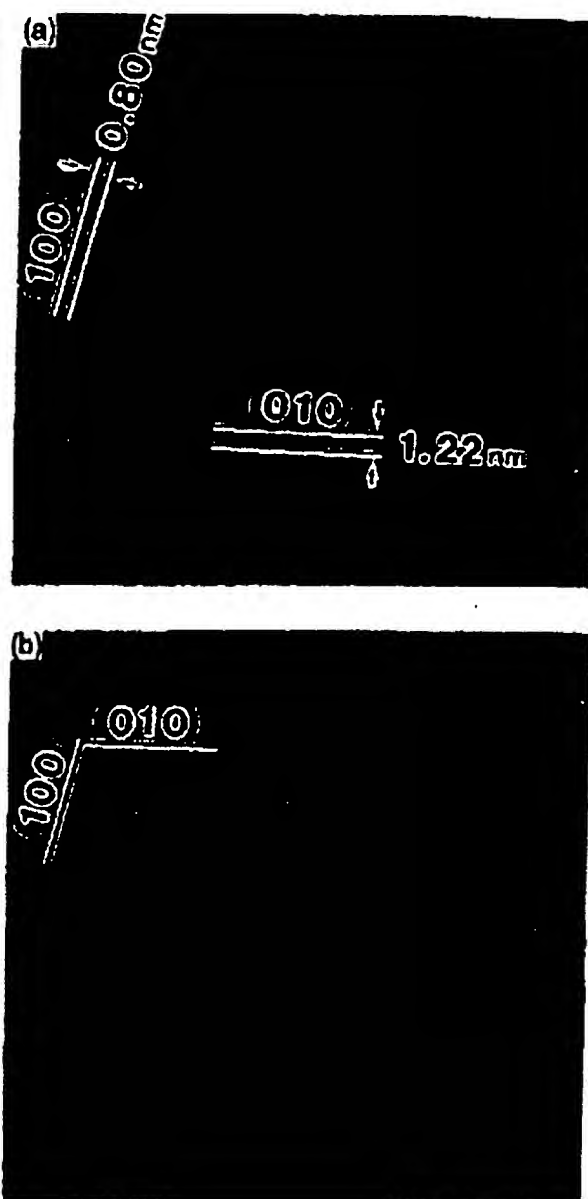


FIG. 4. (a) HREM image of the ulexite grain and (b) FFT filtered image of (a).

planes inside the crystal. Figure 5 also reveals that the individual bundle consists of a single crystal, which was not known for a long time.<sup>13</sup> According to the diffraction patterns of 1-3, the grain boundaries between grains 1 and 2, 2 and 3 are found to be small-angle tilt grain boundaries with a misorientation of  $3^\circ$ . Similarly from the diffraction pattern of 4 and 5, the grain boundary between grains 4 and 5 is a small-angle tilt boundary.



FIG. 5. CTEM bright-field micrograph of ulexite. The diffraction patterns have been obtained from the pointed area.

larities of grains 3 and 4, 5 and 6 are large-angle boundaries with the misorientation of  $30^\circ$  and  $41^\circ$ , respectively. These large-angle boundaries correspond to residual grain, as shown in Fig. 2.

TEM image of a small-angle grain boundary is shown in Fig. 6. This image was taken with the incident beam parallel to the  $[001]$  direction, and the  $(100)$  planes can be observed. The misorientation of the planes across the grain boundary is  $11^\circ$ . Misfit dislocations with the Burgers vector perpendicular to the plane can be introduced at the boundary, although stacking faults cannot be observed because of the lack of quality. The presence of a number of small-angle boundaries is one of the characteristics of

preferred misorientation angles<sup>14</sup> may be coming from the grain boundary relationship because of the atomistic scale matching of the grain boundary usually decreases the grain boundary energy even in the high-angle grain

expected from the streak along the  $(010)$  direction. Another characteristic of ulexite is the presence of lots of stacking faults on the  $(010)$  planes, as shown in Fig. 7. Figure 8(a) is a HREM micrograph and a FFT image observed along the  $[001]$  direction, showing the high density of stacking faults on the  $(010)$  planes. Since the interplanar spacing of  $(010)$  planes is small, the stacking fault energy is considered to be relatively low. Thus, it is concluded that the small-angle grain boundary and stacking fault in one bundle grain would affect the optical properties of ulexite. These defects may lead to reduce the total reflection rate, resulting in a decrease in transparency in the ulexite.

Regarding the high-angle boundary, the distribution of misorientation angles can be measured by SEM-EBSD, as shown in Fig. 2. There is a tendency for the misorientation angle ( $30, 45, 53, 73, 105^\circ$ ) at the interface of the grain boundary, as shown in Fig. 9(a). These

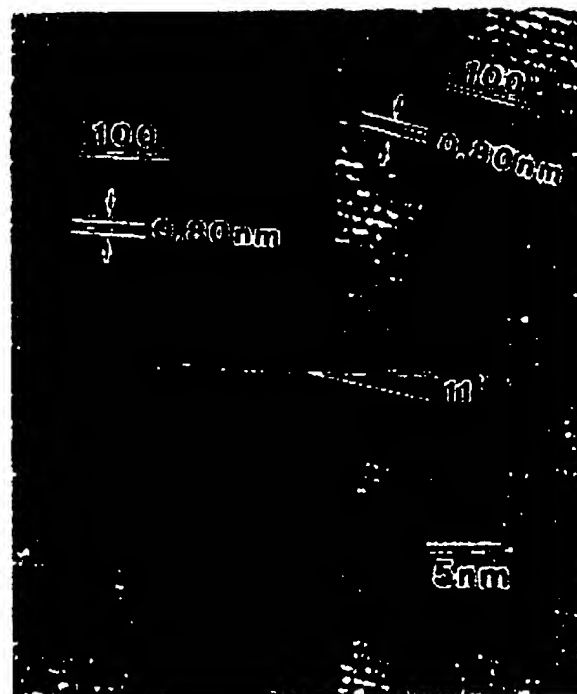


FIG. 6. Lattice image of a small-angle grain boundary. Both sides of the planes are parallel to the  $(100)$  plane. The misorientation of the  $(100)$  planes across the grain boundary is  $11^\circ$ .

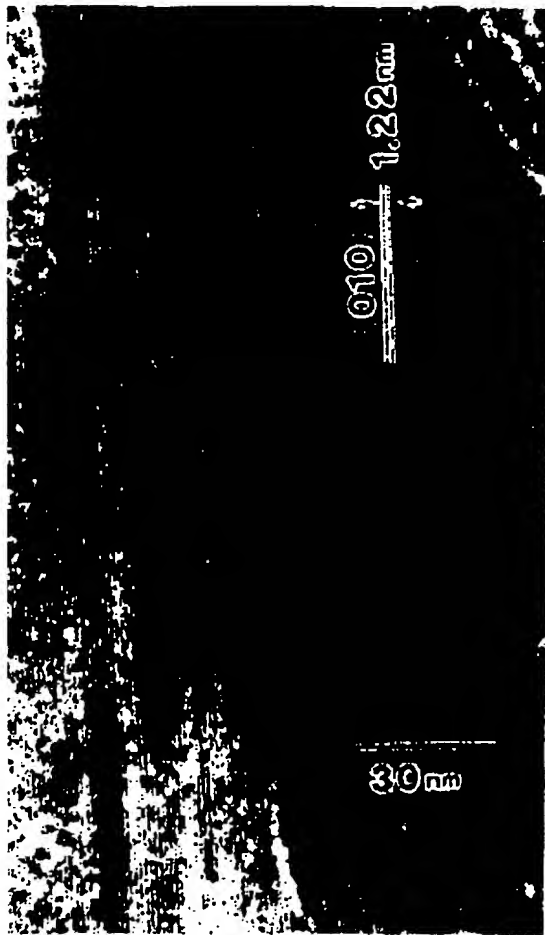


Fig. 7. CTEM micrograph of the stacking faults along the {010} planes in ulexite.

boundary. Thus, the degree of coincidence of atomistic lattice at the grain boundary was calculated as mentioned above, and was compared with the results from the microstructure measurement.

When two sheets of circle plane consisting of 2000 lattice points of the projected unit cell of ulexite superimpose and one of the two rotates around the axis perpendicular to the lattice plane, many lattice points of the planes can superimpose on each other, depending on the rotation.<sup>15,16</sup> For instance, we assume that a constant number of the spheres lies at the lattice point and the one rotates  $1^\circ$  of steps. Each sphere in the two planes overlaps at the certain rotated angle. The degree of coincidence is calculated as the integrated overlapping number of spheres at all lattice points. Figure 9(b) shows the calculated results of the degrees of coincidence at the interface of the grains as a function of the rotation angle. The degrees of the coincidence of the lattice are around  $45^\circ$ .

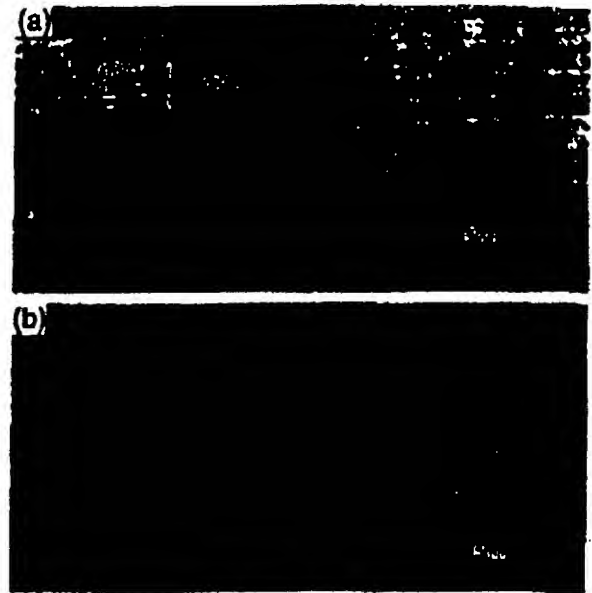


Fig. 8. (a) HREM image and (b) FFT filtered image of the stacking faults along the {010} planes in ulexite.

$75^\circ$ ,  $105^\circ$ , and  $135^\circ$ , which is in good agreement with the distribution results of the microstructure observation as shown in Fig. 9(a). This result indicates that the two grains contact with the preferable plane of high matching probability. Murdoch reported the ulexite crystal is randomly aligned along the *c*-axis.<sup>3</sup> Since there are plenty of planes that have a high degree of coincidence of the lattice for ulexite as shown in Fig. 9(b), the interface of the two grains seems to be a randomly contacted. In this research, controversially, we have found that there is a preferential misorientation angle at the interface of the two grains.

In Fig. 9, each grain adjoins at the grain boundary with high degree of coincidence. These orientation relationships at the grain boundary affect the overall light transmission of each fiber because the light transmission of an individual fiber is influenced by the number of rays reflected at the grain boundary. Thus, comparing to the random orientated grain boundary, the grain boundary with a high degree of coincidence could strongly affect the transmission of fiber.

Furthermore, since there are many preferential misorientation angles at the interface of grains in ulexite, each grain could keep from the grain growth because they maintain the interfacial energy as low as possible to form the certain angle. Therefore, the high degree values of coincidence in the several misorientation angles at the grain boundary as shown in Fig. 9(b) result in the promotion of formation of the small fiber bundle along

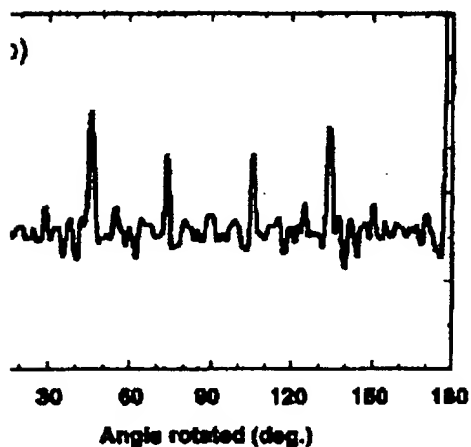
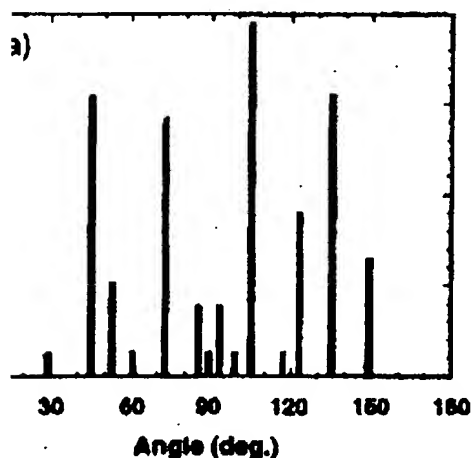


Figure 3) distribution of misorientation angles measured in SEM  
Figure 4) computed relation between the degree of coincidence rotation angle.

reaction to decrease the interfacial energy, as shown in Fig. 2.

## DISCUSSION

The microstructures of ulexite were examined using TEM and CTEM, and the following results were

(1) HREM images of ulexite were successfully observed by using very low electron dose technique.

(2) Each grain with the size of  $10\ \mu\text{m}$  is composed of single crystal plates which pile up in the grain with a small misorientation.

(3) There is a preferable contact angle between two grains at the interface. The experimental results are in good agreement with the simulated results, which indicates the degree of coincidence of the lattice developed the strength of the high-angle grain boundary.

(4) Cleavage planes were determined as (010) in ulexite and stacking faults are also introduced in the plane.

(5) There are a number of small-angle grain boundaries with the misorientation angles between  $3$  and  $11^\circ$ .

(6) Light transmittance would depend on the microstructural characteristic, such as stacking faults and the small-angle grain boundaries.

## ACKNOWLEDGMENTS

This work was promoted by AIST, MITI, Japan as part of the Synergy Ceramics Project under the Industrial Science and Technology Frontier (ISTF) program. Under this program, part of the work was supported by NEDO. The authors are members of the Joint Research Consortium of Synergy Ceramics.

## REFERENCES

1. N. Kreidl, *Ceram. Bull.* **63**, 1394 (1984).
2. M. A. Saifi, S. J. Jong, L. G. Cohen, and J. Stone, *Opt. Lett.* **7**, 43 (1982).
3. H. Ezkorn and W. E. Heinlein, *Electron. Lett.* **20**, 423 (1984).
4. E. Mackawa and S. Sumida, *J. Lightwave Technol. Lett.* **3**, 829 (1985).
5. J. Murdoch, *Am. Mineral.* **25**, 754 (1940).
6. E. J. Weichel-Moore and R. J. Potter, *Nature* **200**, 1163 (1963).
7. G. S. Baur and L. B. Sand, *Am. Mineral.* **42**, 676 (1957).
8. J. R. Clark and C. L. Christ, *Am. Mineral.* **44**, 712 (1959).
9. J. R. Clark and D. E. Appleman, *Science* **145**, 1295 (1964).
10. L. Stoch and I. Wacławski, *J. Therm. Anal.* **36**, 2045 (1990).
11. C. L. Christ, *Am. Mineral.* **45**, 334 (1960).
12. C. L. Christ and J. R. Clark, *Phys. Chem. Minerals* **2**, 59 (1977).
13. S. Ghose, C. Wan, and J. R. Clark, *Am. Mineral.* **63**, 160 (1978).
14. S. Sueo, H. Takoda, and R. Sakaguchi, *Mineral. J.* **6**, 172 (1971).
15. Z. Inoue, Y. Uemura, and Y. Inomata, *J. Mater. Sci.* **16**, 2297 (1981).
16. Y. Uemura, Y. Inomata, and Z. Inoue, *J. Mater. Sci.* **16**, 2333 (1981).